

# Differential cross sections for elastic electron scattering. II. Charge cloud polarization in N<sub>2</sub>

D. Herrmann, K. Jost, and J. Kessler

*Physikalisches Institut, Westfälische Wilhelms Universität, Münster, Germany*

M. Fink

*Physics Department and Electronics Research Center, University of Texas, Austin, Texas 78712*

(Received 11 December 1974)

Relative elastic differential cross sections for electron scattering from N<sub>2</sub> molecules have been measured with a crossed beam technique in order to investigate the influence of charge cloud polarization. The angular range studied was 3–135 deg and the electron energies were between 90 and 1000 eV. Comparison with theoretical calculations based on the independent atom model using partial wave atomic scattering factors shows strong deviations at small scattering angles. This discrepancy is discussed from the point of view of charge cloud polarization. It is found that calculations including an additional polarization potential improve the theoretical description of the experimental small angle data.

## I. INTRODUCTION

This work forms part of a series of electron scattering experiments<sup>1</sup> in which relative elastic differential cross sections  $\sigma(\theta)$  have been measured in order to investigate the effect of charge cloud polarization. Under the influence of the incoming electron the target atom can be considered as an induced dipole<sup>2</sup> with a potential  $V_{\text{pol}}$  proportional to  $r^{-4}$  for large  $r$ . This charge cloud polarization should mainly influence electrons which are scattered through small angles (i.e., in the classical picture, electrons which have large impact parameters), whereas at large angles a Hartree-Fock potential should be sufficient to determine the cross sections reliably. Therefore, the experimental data, which have been taken between 3° and 135°, have been fitted at large angles to the cross sections which have been calculated by the partial wave method using a static potential. Thus the data were normalized to an absolute scale.<sup>3</sup> The energies of the incoming electrons have been varied between 90 and 1000 eV in order to study the energy dependence of the charge cloud polarization.

## II. EXPERIMENTAL METHOD

A detailed description of the apparatus and a complete error analysis are given in Ref. 1. Therefore the experimental method is only briefly discussed here.

Electrons from a rotatable electron gun with a tungsten hairpin cathode were scattered by N<sub>2</sub> molecules, which were formed to a beam by a small capillary in the axis of rotation of the electron gun. The scattered electrons were energy analyzed by a filter lens, which eliminated electrons having excited electronic transitions of the molecule. Electrons with energy losses corresponding to vibrational and rotational excitations only were not suppressed. Ions were removed from the beam before the electrons finally reached the collector. The contribution of the background gas to the scattered intensity was determined by means of a second nozzle offside the electron beam and equivalent to the first one. The difference of the scattered intensities

with the first and the second nozzle in operation yielded the quantity  $\sigma(\theta)$  to be studied. The scattered intensities were recorded at  $+\theta$  and  $-\theta$  in order to check for symmetry and to determine  $\theta = 0^\circ$ . The N<sub>2</sub> gas had a purity of 99.999%. The relative error of the shape of the cross section is  $\pm 5\%$  in the angular range  $25^\circ \leq \theta \leq 135^\circ$  and additionally 6% at smaller angles (cf. Ref. 1).

## III. ANALYSIS OF THE DATA USING THE INDEPENDENT ATOM MODEL

The relative cross sections measured could be brought up to an absolute scale by fitting the experimental data to theoretical results<sup>3</sup> using the independent atom model<sup>4</sup> (IAM) together with partial wave scattering factors of atomic nitrogen by Fink and Yates<sup>5</sup> and by Fink and Ingram.<sup>6</sup> In the special case of N<sub>2</sub> the molecular differential cross section  $\sigma_M(\theta)$  is given by

$$\sigma_M(\theta) = 2\sigma_A(\theta) \cdot (1 + \sin sr_0/sr_0) \quad (1)$$

( $s = 2k \sin \frac{1}{2}\theta$ ,  $k = 2\pi/\lambda$  = wavenumber of the incoming electron,  $r_0$  = most probable separation of the N nuclei taken as 1.0976 Å,  $\sigma_A(\theta)$  = atomic cross section,  $\theta$  = scattering angle). The IAM neither takes into account any redistribution of atomic electrons due to molecular binding<sup>7</sup> nor multiple scattering within the molecule.<sup>8,9</sup> Nevertheless good agreement between IAM calculations and many scattering experiments with electron energies in the discussed energy range has been reported,<sup>10,11</sup> at least at larger angles.

Also in the present case the simple IAM succeeds at large angles in describing the results obtained. This can be seen as follows: The IAM cross sections as given by Eq. (1) differ from the cross section of two single atoms by a factor of  $1 + (\sin sr_0/sr_0)$ . It seems to be a good test of the IAM to compare the theoretical interference term  $1 + (\sin sr_0/sr_0)$  with the ratios  $\sigma_M(\theta)/2\sigma_A(\theta)$  where  $\sigma_M(\theta)$  is the experimental cross section and  $\sigma_A(\theta)$  the theoretical atomic cross section. Figure 1 shows for three typical energies that good agreement of  $\sigma_M(\theta)/2\sigma_A(\theta)$  and  $1 + (\sin sr_0/sr_0)$  is found for angles larger than 30°. In comparing these curves one must bear in mind the experimental error and the magnitude

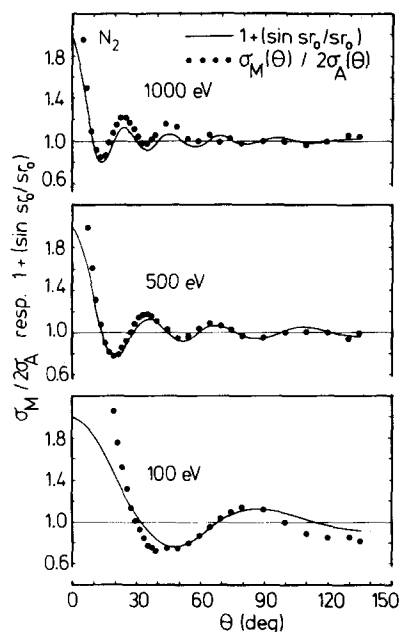


FIG. 1. Molecular interferences in  $N_2$  for three typical energies. Comparison of  $\sigma_M(\theta)/2\sigma_A(\theta)$  with the theoretical curve  $1 + (\sin sr_0/sr_0)$ .

of the interference amplitudes, which are only a few percent of the molecular cross section in the range of large angles. Furthermore  $\sigma_M(\theta)/2\sigma_A(\theta)$  depends also on the quality of the theoretical values for  $\sigma_A(\theta)$ .

At small angles the experimental values exceed the values of  $1 + (\sin sr_0/sr_0)$ . The reason is discussed later.

Table I gives our experimental cross sections. These values have been obtained by fitting the relative experimental cross sections to the theoretical IAM calculations at  $\theta = 90^\circ$  at each energy.<sup>12</sup> This large angle must be chosen, because the theoretical atomic scattering factors were calculated using a Hartree-Fock potential where exchange of the incoming electron with the atomic electrons and polarization of the charge cloud, which influence mainly electrons scattered by small angles, were neglected. Figure 2 shows that no appreciable error is caused by fitting at  $90^\circ$ : Within a wide angular range ( $\theta \geq 30^\circ$ ), the ratio  $\sigma(\theta)_{\text{exp}}/\sigma(\theta)_{\text{IAM}}$  is nearly unity, which means that the shape of the ex-

TABLE I. Experimental cross sections for elastic electron scattering from  $N_2$  in units of  $\text{\AA}^2$ . These values have been obtained by fitting the relative experimental data to IAM calculations without charge cloud polarization at  $\theta = 90^\circ$ . cf. Table II for fitting to absolute measurements.

$\theta$ (deg)	90 eV	100 eV	150 eV	200 eV	300 eV	400 eV	500 eV	600 eV	800 eV	1000 eV
3	...	42	36	38	30	30	24	21	19.7	19.0
4	32	37	32	32	25	24	19.3	17.4	16.7	16.9
5	27	32	28	28	21	21	16.2	14.7	13.3	12.5
6	25	29	25	23	17.9	17.3	13.6	11.9	10.6	9.9
7	22	25	23	20	15.3	14.4	11.2	9.9	8.4	7.4
8	20	23	19.6	17.2	12.8	11.3	9.0	7.9	6.8	5.7
9	18.1	19.9	17.4	14.6	11.1	9.8	7.3	6.2	5.0	4.1
10	16.1	17.4	14.2	12.5	9.2	8.1	6.0	5.0	3.8	3.0
12	13.1	13.5	11.0	9.2	6.4	5.2	3.9	3.1	2.3	1.81
14	10.5	10.3	8.5	6.7	4.5	3.5	2.5	1.98	1.45	1.18
16	8.2	7.8	6.3	4.8	3.1	2.4	1.64	1.29	0.99	0.86
18	5.8	6.2	4.8	3.4	2.1	1.62	1.14	0.93	0.76	0.70
20	5.0	4.8	3.5	2.5	1.50	1.15	0.85	0.72	0.63	0.55
22	4.0	3.6	2.6	1.79	1.07	0.88	0.68	0.61	0.52	0.44
24	3.1	2.8	1.98	1.35	0.83	0.71	0.57	0.52	0.44	0.36
26	2.5	2.2	1.50	1.04	0.66	0.60	0.49	0.45	0.36	0.27
28	1.90	1.63	1.14	0.80	0.54	0.52	0.43	0.38	0.29	0.20
30	1.50	1.27	0.90	0.65	0.47	0.45	0.37	0.33	0.23	0.155
32	1.20	1.02	0.71	0.54	0.42	0.42	0.33	0.27	0.178	0.118
34	0.96	0.81	0.59	0.46	0.38	0.36	0.28	0.23	0.143	0.092
36	0.78	0.65	0.49	0.40	0.34	0.32	0.24	0.183	0.111	0.076
38	0.65	0.55	0.42	0.35	0.31	0.27	0.197	0.150	0.090	0.066
40	0.52	0.46	0.37	0.33	0.28	0.24	0.163	0.124	0.076	0.059
45	0.38	0.33	0.29	0.27	0.22	0.164	0.108	0.077	0.056	0.045
50	0.28	0.24	0.24	0.22	0.163	0.112	0.075	0.058	0.043	0.031
55	0.22	0.187	0.20	0.188	0.119	0.081	0.060	0.048	0.033	0.021
60	0.170	0.153	0.173	0.156	0.090	0.066	0.051	0.039	0.024	0.0160
65	0.138	0.133	0.152	0.129	0.072	0.057	0.043	0.031	0.0180	0.0134
70	0.123	0.119	0.132	0.107	0.063	0.051	0.036	0.024	0.0148	0.0109
75	0.110	0.111	0.115	0.089	0.057	0.043	0.029	0.0189	0.0128	0.0086
80	0.104	0.108	0.105	0.078	0.054	0.038	0.023	0.0160	0.0108	0.0069
90	0.104	0.110	0.092	0.069	0.047	0.027	0.0178	0.0139	0.0077	0.0052
100	0.120	0.118	0.091	0.070	0.040	0.023	0.0153	0.0111	0.0060	0.0040
110	0.152	0.132	0.097	0.074	0.034	0.021	0.0129	0.0085	0.0052	0.0032
120	0.191	0.160	0.108	0.078	0.031	0.020	0.0111	0.0076	0.0044	0.0028
130	0.23	0.198	0.127	0.079	0.031	0.0190	0.0101	0.0072	0.0038	0.0025
135	0.25	0.21	0.127	0.077	0.031	0.0181	0.0095	0.0069	0.0036	0.0024

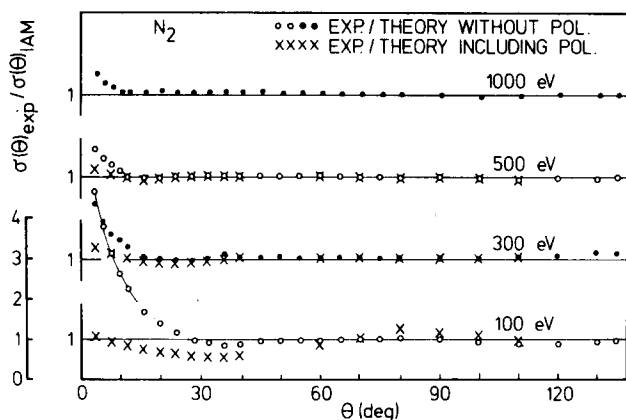


FIG. 2. Comparison of experimental cross sections with theory.  $\bullet\bullet\bullet$  IAM calculations without charge cloud polarization,  $\times\times\times$  IAM calculations using atomic scattering factors which include charge cloud polarization. The experimental values have been normalized at  $\theta=90^\circ$  to the IAM calculations without charge cloud polarization.

perimental and theoretical IAM cross sections are the same. Small deviations within a few percent from unity may be caused by the experimental error and by the deficiencies of the IAM and/or the theoretical atomic cross sections. However at small angles large deviations between IAM calculations and the experimental cross sections were found: At 100 eV and  $\theta=4^\circ$  the experimental cross section exceeds the IAM value by a factor of 4.5, at 500 eV by a factor of 1.7, and at 1000 eV still by a factor of 1.5. The reason for this strong discrepancy is discussed in Sec. V.

#### IV. COMPARISON WITH OTHER EXPERIMENTS; TOTAL ELASTIC CROSS SECTIONS

In Fig. 3 our data are compared with several other experiments. Within the combined experimental er-

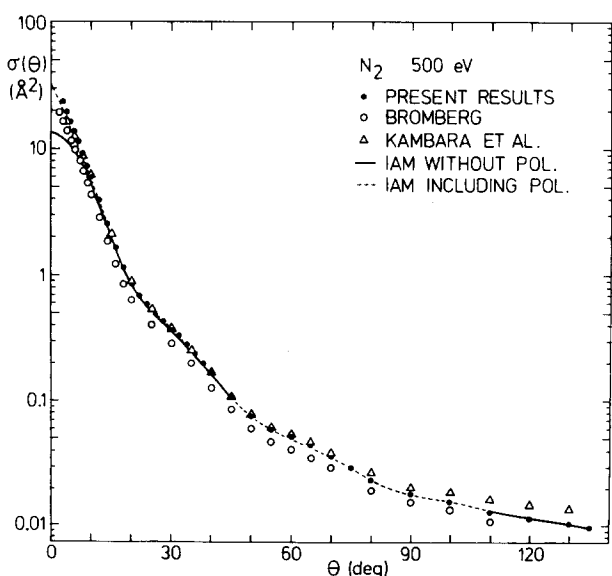


FIG. 3. Cross sections at 500 eV. The diagram shows several experimental data together with theoretical calculations. Our data are shown as listed in Table I. The results of Kambara *et al.* are fitted at  $\theta=30^\circ$  to our results.

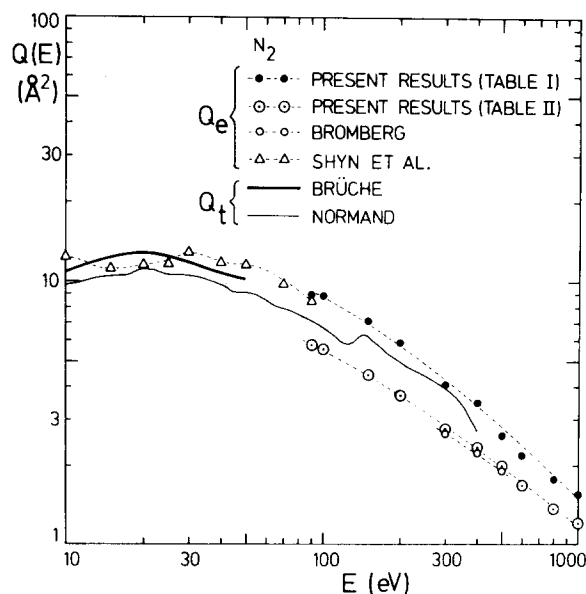


FIG. 4. Experimental results of total collision cross sections  $Q_t$  (—) and total elastic cross sections  $Q_e$  (---) vs energy.

rors our cross sections agree in shape with those of Bromberg<sup>13,14</sup> (absolute) and Jansen *et al.*<sup>15</sup> (calibrated among themselves and normalized to Bromberg's results). There is also agreement with the experimental cross sections of Kambara and Kuchitsu<sup>16</sup> (relative, in Fig. 3 fitted to our results at  $\theta=30^\circ$ ) except for the data at 500 eV at large angles ( $\theta \geq 80^\circ$ ), where our results are about 30% smaller. The cross sections at 90 eV have been compared with the relative measurements of Shyn *et al.*<sup>17</sup> If fitted at  $\theta=30^\circ$ , our small angle data ( $\theta \leq 15^\circ$ ) are more than 30% smaller and our large angle data ( $\theta \geq 60^\circ$ ) about 30% larger than the cross sections of Shyn *et al.* Apart from this discrepancy, it should be pointed out here that it is very satisfactory that the shapes of the cross sections obtained by several different investigators using different techniques agree in most cases within experimental errors.

As explained above, the shapes of our cross sections agree well with many other experimental results. However, we found a slightly energy dependent difference of about 30% between the absolute values of our data (fitted to theory at  $90^\circ$ ; Table I) and those measured by Bromberg<sup>14</sup> and by Jansen *et al.*<sup>15</sup> This means that at large angles the theoretical IAM cross sections exceed the absolute experimental data in the energy range investigated. In order to make our data consistent with the absolute measurements,<sup>14,15</sup> one has to multiply the values of Table I with the conversion factors listed in Table II. These slightly energy dependent conversion factors have been obtained by fitting our values in the angular range from  $\theta=10^\circ$  to  $30^\circ$  to those of Bromberg<sup>14</sup> and Jansen *et al.*<sup>15</sup> A few values had to be either interpolated or extrapolated.

Because of the large angular range covered by our experiment, it is possible to determine total elastic cross sections  $Q_e$  by graphical integration of curves  $2\pi\sigma(\theta)\sin\theta$  vs  $\theta$ , where the factor  $2\pi$  originates from

TABLE II. Conversion factors. Multiply the cross sections of Table I by the factors given below in order to get consistency with recent absolute measurements.<sup>a</sup> Values obtained are in units of Å<sup>2</sup>. Factors given in parenthesis are either interpolated or extrapolated.

Energy	90 eV	100 eV	150 eV	200 eV	300 eV	400 eV	500 eV	600 eV	800 eV	1000 eV
Factor	(0.65)	0.63	0.62	0.63	0.67	0.67	0.76	(0.77)	(0.77)	0.78

<sup>a</sup>Reference 14 and 15.

the azimuthal integration. The values outside the angular range covered by our experiment could be extrapolated with reasonable reliability. The relative error of the integration is estimated to be smaller than 3%. The results are shown in Fig. 4 for both our fitting procedures, i. e., fitting to theory (Table I) and fitting to absolute experiments (Table II). For comparison, the graphical integration has also been applied to Bromberg's results.<sup>14</sup> As expected from the above discussion, our results on the basis of Table II agree within experimental error with those of Bromberg, whereas our results from Table I are about 30% higher. Figure 4 also shows for comparison total collision cross sections  $Q_t$  as measured by Brueche<sup>18</sup> and Normand,<sup>19</sup> where the data of Brueche should be considered to be the more reliable ones.<sup>20</sup> Because the total collision cross section  $Q_t$  contains both elastic and inelastic processes, it must be larger than the total elastic cross section  $Q_e$ . However, our  $Q_e$  values computed by means of Table I are even larger than the absolute values of  $Q_t$ , whereas the  $Q_e$  values according to Table II behave as expected. This means that the fitting of our data according to Table II is consistent with the existing absolute measurements and that the values given in Table I are most probably too high. By the same argument the total elastic cross sections given by Shyn *et al.*<sup>17</sup> are also

too high. Nevertheless, the conclusions drawn in the next section do not depend on whether Table I or Table II is used, because for these considerations the shape of the curves is more important than their absolute value.

## V. COMPARISON OF THE SMALL ANGLE DATA WITH THEORY; CONCLUSIONS

As shown in Figs. 1, 2, and 3 the experimental cross sections in the small angle range (ca.  $30^\circ > \theta > 3^\circ$ ) are much larger than those calculated with the IAM. This cannot be explained by the experimental uncertainties. Neither are the discrepancies due to multiple scattering within the molecule, as an estimate shows,<sup>9</sup> nor to exchange, since Walker<sup>21</sup> showed for rare gases that exchange does not appreciably change the calculated small angle cross sections for energies higher than 100 eV.

The differences are mainly caused by neglecting charge cloud polarization in the atomic scattering factors. This becomes evident, when the shape of the small angle cross sections is considered (Fig. 5). As in our other scattering experiments with different targets<sup>1</sup> or recent experiments of other authors,<sup>13-15,22,23</sup> the small angle cross sections of N<sub>2</sub> can be approximated by an exponential function. Figure 6 shows that in a diagram of the cross section vs the momentum transfer  $s$  the data at all energies converge to one curve

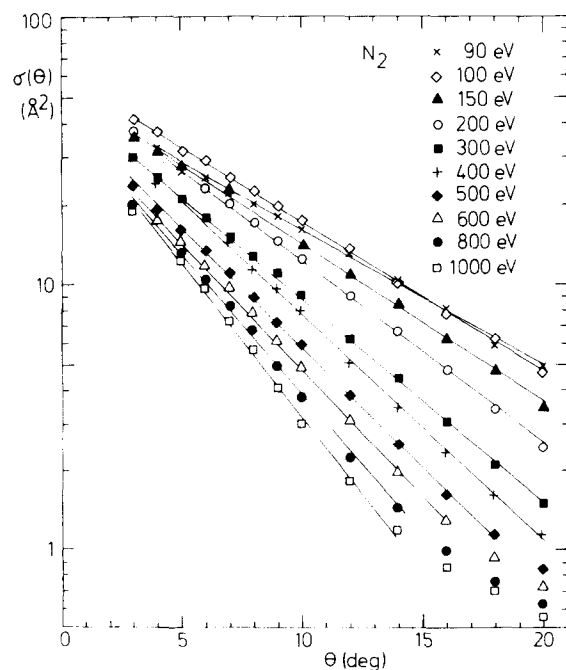


FIG. 5. Experimental cross sections as listed in Table I in the small angle range. The straight lines show the exponential behavior of the data at these angles.

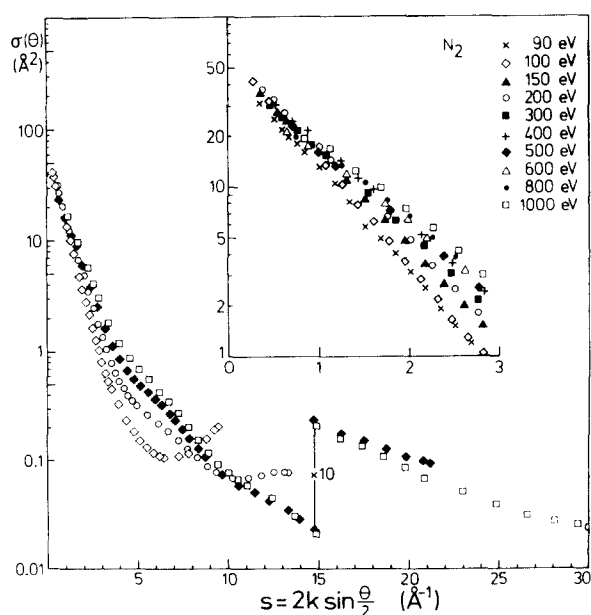


FIG. 6. Cross sections as listed in Table I as a function of the momentum transfer  $s$ . The insert shows details for small values of  $s$ .

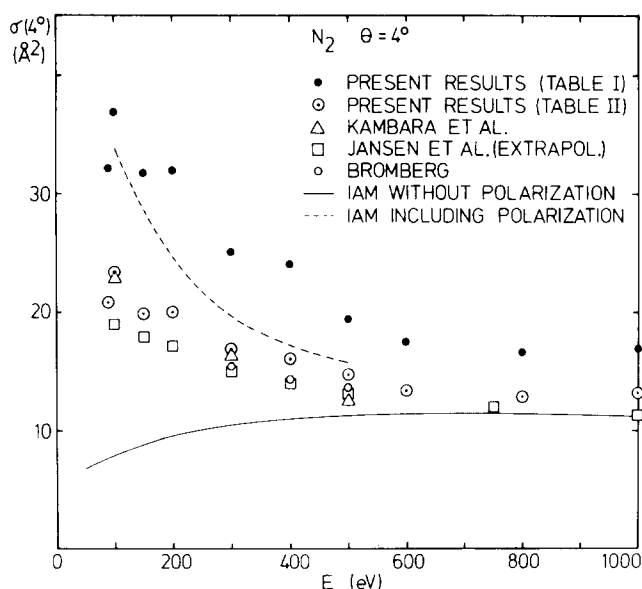


FIG. 7. Experimental and theoretical cross sections at  $\theta = 4^\circ$  as a function of energy. Results of Kambara *et al.* fitted to absolute measurements at  $\theta = 30^\circ$ .

for small  $s$ . This is a necessary condition of the validity of Born's first approximation. Assuming the Born approximation to be correct, this exponential behavior leads to a scattering potential, which has asymptotically the form of a polarization potential:

$$V(r) = \pm 4cb / [\pi(r^2 + b^2)^2] \quad (2)$$

( $c$ ,  $b$  constant).<sup>22</sup>

A more sophisticated method has been developed by Konaka and Kohl,<sup>24</sup> who employed the second Born approximation to derive an effective polarization potential which satisfies also the  $r^{-4}$  behavior for large  $r$  [similar to Eq. (2)], but with the advantage that it includes a non-adiabatic correction. Using this potential, differential cross sections of  $N_2$  for 100, 300, 400, and 500 eV have been calculated on the basis of the IAM. In Figs. 2 and 3 these theoretical values are also compared with our experimental results. Apart from a slight modification at 100 eV, inclusion of this effective polarization potential does not affect the cross sections at medium or large angles, whereas at small angles it improves the agreement between experimental and theoretical results considerably.

The typical energy dependence of the small angle data is illustrated in Fig. 7, where the theoretical and experimental cross sections at  $\theta = 4^\circ$  are shown as a function of the scattering energy. At this angle the theoretical cross sections without polarization remain nearly constant, whereas the experimental cross sections as well as the theoretical cross sections including polarization increase with decreasing energy below 600 eV. This indicates that at this angle charge cloud po-

larization becomes in the case of  $N_2$  important for energies smaller than 600 eV. On the whole there is an analogous influence of charge cloud polarization on  $N_2$  as it is on the rare gases and the  $H_2$  molecule.<sup>1</sup>

## ACKNOWLEDGMENTS

One of us (M. F.) is indebted to the Westfälische Wilhelms Universität for the warm hospitality while the experimental portion of the work was carried out. We would also like to acknowledge the support of the "Deutsche Forschungsgemeinschaft."

- <sup>1</sup>M. Fink, K. Jost, and D. Herrmann, Phys. Rev. (to be published). Apart from the results on  $H_2$  presented there, further results on He, Ne, Ar, Kr, Xe,  $C_2H_2$ ,  $C_2H_4$ , and  $C_2H_6$  are being prepared for publication.
- <sup>2</sup>H. S. W. Massey, E. H. S. Burhop, and H. B. Gilbody, *Electronic and Ionic Impact Phenomena* (Clarendon, Oxford, 1969), Vol. I, p. 509.
- <sup>3</sup>It should be noted that this procedure depends on the reliability of the theoretical calculations; it would therefore be subject to corrections, if the theoretical data would be improved. Fitting is also possible to absolute measurements; cf. Sec. IV of the text.
- <sup>4</sup>H. S. W. Massey, E. H. S. Burhop, and H. B. Gilbody, in Ref. 2, Vol. II, p. 666.
- <sup>5</sup>M. Fink and A. C. Yates, "Tables of Scattering Amplitudes and Spin Polarizations," Technical Report No. 103, 1 March 1971, The University of Texas at Austin.
- <sup>6</sup>M. Fink and J. Ingram, At. Data 4, 129 (1972).
- <sup>7</sup>M. Fink, R. A. Bonham, and D. A. Kohl, Chem. Phys. Lett. 4, 349 (1969).
- <sup>8</sup>Molecular vibrations need not be taken into account, because the modifications due to vibrations are smaller than the experimental accuracy. Multiple scattering was calculated with the eikonal approximation<sup>9</sup> and found to be less than 1% of  $\sigma_A$ .
- <sup>9</sup>H. Tuley, thesis, Phys. Dept., University of Texas, 1973.
- <sup>10</sup>J. Kessler, Rev. Mod. Phys. 41, 3 (1969).
- <sup>11</sup>J. Kessler, J. Lorenz, H. Rempp, and W. Bühring, Z. Phys. 246, 348 (1971).
- <sup>12</sup>As we had no theoretical atomic scattering factors for the energy 90 eV, we interpolated here  $\sigma_A(90^\circ)$  between 75 and 100 eV.
- <sup>13</sup>J. P. Bromberg, J. Chem. Phys. 50, 3906 (1969).
- <sup>14</sup>J. P. Bromberg, J. Chem. Phys. 52, 1243 (1970).
- <sup>15</sup>R. H. J. Jansen, F. J. de Heer, H. J. Luyken, B. van Wingerden, and H. J. Blaauw, FOM report, FOM-nr. 35693, Amolf 74/133, May 1974, Amsterdam, Netherlands, 1974.
- <sup>16</sup>H. Kambara and K. Kuchitsu, Jap. J. Appl. Phys. 11, 609 (1972).
- <sup>17</sup>T. W. Shyn, R. S. Stolarksi, and G. R. Carignan, Phys. Rev. A 6, 1002 (1972).
- <sup>18</sup>E. Brueche, Ann. Phys. (Leipz.) 82, 912 (1927).
- <sup>19</sup>C. E. Normand, Phys. Rev. 35, 1217 (1930).
- <sup>20</sup>B. Bederson and L. J. Kieffer, Rev. Mod. Phys. 43, 601 (1971).
- <sup>21</sup>D. W. Walker, Adv. Phys. 20, 257 (1971).
- <sup>22</sup>J. P. Bromberg, J. Chem. Phys. 51, 4117 (1969).
- <sup>23</sup>J. P. Bromberg, J. Chem. Phys. 61, 963 (1974).
- <sup>24</sup>S. Konaka and D. A. Kohl, preprint, 1974.